Splice Connections for Built-Up Column Assemblies in Cold-Formed Steel Construction

Sivaganesh Selvaraj, Ph.D.[1]; and Mahendrakumar Madhavan, Ph.D., P.E., M.ASCE[2]

Abstract: The development of simple connection methods is necessary for increasing cold-formed steel (CFS) construction activities. A new splice connection concept for the CFS built-up column-to-column connections is presented in this paper. This simple connection concept will use the same size and shape of the geometry as the CFS built-up column, which will enable a quick erection process. The new splice connection configurations, arrangement, and installation methods for cold-formed steel construction are demonstrated. Twenty-eight experiments, which include four actual columns, two disconnected columns, and 22 columns with splice connections, are carried out. This paper examines the influence of various parameters of splice connections such as length, thickness, and number of fastener rows. The design strength of the actual column is determined using the direct strength method (with modified global and local slenderness approaches) and is compared with the results of the splice connected columns for adequacy. The force transfer mechanism and failure modes of splice connection components are demonstrated in the form of detailed sketches. The smaller length splice connections led to localized failures, while the longer splice connections enabled the uniform force distribution between the built-up column cross-sections. Finally, it is recommended that the splice connection configuration should be a minimum of 300 mm in length, the splice thickness should be equal to the CFS built-up cross-section, and two rows of fasteners for attaining the required design strength of the built-up column members. **DOI: 10.1061/JSENDH.STENG-11540.** *© 2022 American Society of Civil Engineers.*

Author keywords: Cold-formed steel (CFS); Built-up cross-section column assemblies; Column-column connections; Splice connections; Practical applications; Fastener connections.

Introduction

The evolution of cold-formed steel construction from low- to mid-rise to multihigh-rise structures necessitates built-up cross-section members rather than traditional single sections. In general, the built-up cross-sections are used as corner columns and as intermediate columns at regular spacing in the cold-formed steel (CFS) construction. In Indian construction practice, the column-to-column connections are avoided at the floor level and at the vicinity of the beam-column connections to prevent column failure (strong column weak beam). Typical, splice, and end-plate connections used in hot-rolled steel construction [Figs. 1(a–h)] will not apply to the CFS sections due to the complexity of bolting, welding, and drilling works. The splice connections with unstiffened plain plates [similar to Fig. 1(a)] are currently being employed for CFS built-up assemblies, but there is a vulnerability to buckling of the thin CFS plates. In addition, the column-to-column connections in the built-up assembly of CFS construction shall not have any extrusions or projections beyond the size of the column for the attachment of sheathing boards [Figs. 1(q–u)]. Therefore, the column-to-column connections in the CFS construction shall be simple and aligned with the geometry of the common built-up column assemblies used [Figs. 1(j–p)].

Although a design guide by the National Institute of Standards and Technology (NIST 2016) provides an alternative way to eliminate the column-to-column splice connections in CFS construction, it is necessary to have a specific design guideline for CFS column-to-column connections for unavoidable circumstances. Therefore, this research aims to address the following questions: (1) where to provide the splice connection to achieve the strength and stiffness equal to the normal column; and (2) what is the connection configuration required to uniformly distribute the force, including length of the splice, the thickness of the splice, and a number of fastener connections?

Splice Connection Concept Development for Built-Up Column Assembly

Geometry of the Splice Connection for Built-Up Column Assembly

In this research, simple connection forms are developed for the CFS built-up column-to-column assemblies. The connection forms are developed such that they are the same shape as the built-up column cross-sections and do not create any additional extrusion in the built-up column members to enable sheathing installations. The splice connection configuration was developed simply in both geometries as well as in the installation procedure. This simple splice connection can be provided from inside and outside the built-up cross-section assemblies, as shown in Figs. 2(a and b); however, the inner splice provision will be difficult for installation due to geometric imperfection (deviation from the original shape), difficulty in holding the splice component inside the built-up cross-section during the fastener driven process, and difficulty in marking

[1]Postdoctoral Fellow, Dept. of Civil and Environmental Engineering, The Hong Kong Polytechnic Univ., Hong Kong. ORCID: https://orcid.org/0000-0003-0782-7003. Email: sivaganesh.selvaraj@polyu.edu.hk

[2]Professor, Dept. of Civil Engineering, Indian Institute of Technology Hyderabad, Kandi, Sangareddy, Telangana 502 285, India (corresponding author). ORCID: https://orcid.org/0000-0002-3144-5278. Email: mkm@ce.iith.ac.in

Note. This manuscript was submitted on April 4, 2022; approved on October 7, 2022; published online on December 16, 2022. Discussion period open until May 16, 2023; separate discussions must be submitted for individual papers. This paper is part of the ***Journal of Structural Engineering***, © ASCE, ISSN 0733-9445.

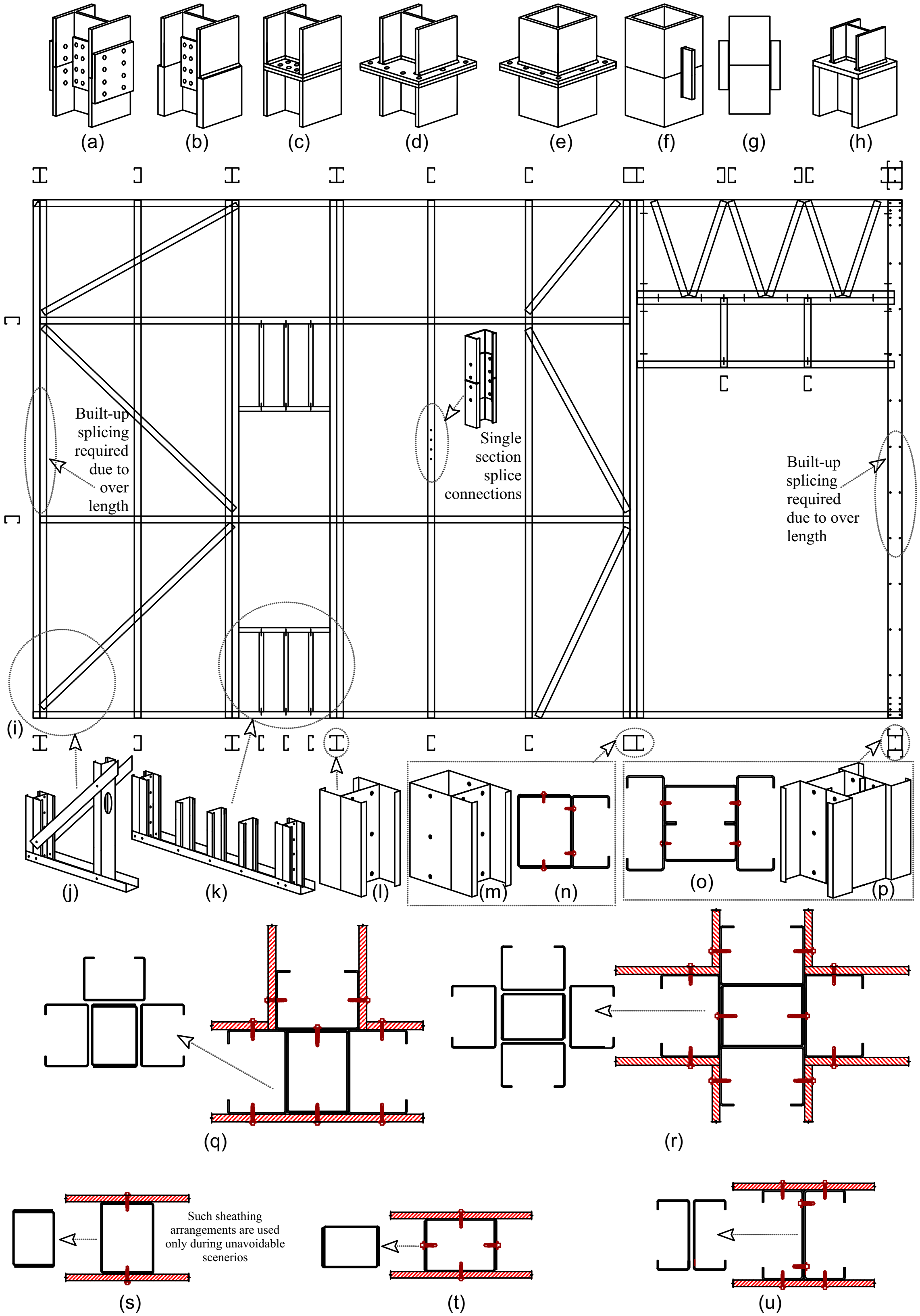

Fig. 1. Traditional column-to-column connections in hot rolled steel members: (a) External cover plate connection for same size columns; (b) internal cover plate connection with welding for different size columns; (c and d) bearing-type end plate connections for I-section columns; (e) bearing-type end plate connections for tubular columns; (f and g) side-plate welded connection for tubular columns; (h) bearing-type base plate connections for changing geometry columns (i) View of CFS wall frame construction with various members and connections; (j) connection between end track and corner column; (k) connection between end track and intermediate columns; (l) back-to-back connected column; (m and n) built-up column with three cross-sections; (o and p) built-up column with four cross-sections; various fastener connections in cold-formed steel construction; and (q–u) connection between sheathed wall-to-wall in cold-formed steel construction.

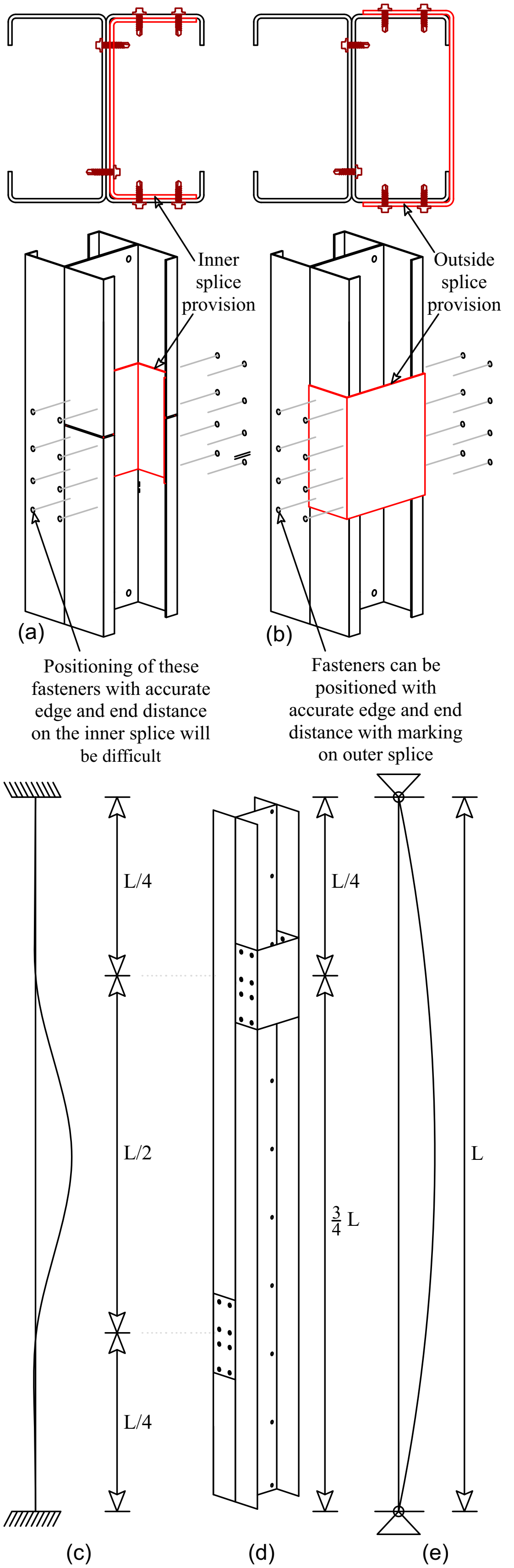

Fig. 2. Possible splice connections in cold-formed steel construction: (a) column-to-column connection with inner splice; (b) column-to-column connection with outer splice; (c) fixed end column deflection shape; (d) appropriate location for the splices; and (e) hinged end column deflection shape.

on the inner splice for accurate fastener edge and end distance to avoid tearing or cleavage failure. Due to these reasons, most of the previous research on the CFS connections used outer splice or outer overlap (Ho and Chung 2006; Zhang and Tong 2008; Dubina and Ungureanu 2010; Liu et al. 2015); it is also an industry preference. Therefore, the outside splice connection method [Fig. 2(b)] was adopted in this present approach for developing a new connection for a built-up column assembly. The connections are developed for three different common forms of CFS built-up column assemblies: (1) back-to-back connected lipped channels [Fig. 3(a)]; (2) back-to-back connected unlipped channels [Figs. 3(b and c)]; and (3) face-to-face connected unlipped channels [Fig. 3(d)]. Geometrically, the developed splice connections can be classified into two categories: same size splices and oversize splices. The oversize splice can be used in the back-to-back (I-shape) connected built-up columns formed from lipped channels [Fig. 3(a)] and face-to-face connected closed cross-section assemblies formed from unlipped channels [Fig. 3(d)], while the same size splice can be used in the back-to-back connected (I-shape) built-up column cross-section assemblies [Figs. 3(b and c)], which are formed by two unlipped channels.

The oversized splice can also be used for the back-to-back connected unlipped I channels [Fig. 3(c)] but only where the individual limbs of built-up members are cut at the same location and need to be connected [depicted in Figs. 4(s–v)]. However, such full-cut splice connections in CFS built-up members are not a preferable practice in the industry due to the uncertainty of achieving full strength and stiffness of the member, and, even though they are all of the same size and shape (four individual limbs, i.e., two each from two built-up sections), the imperfection and end distortion due to handling, lifting, and transportation may make the assembling and connecting critical in the construction site. Nevertheless, the present research attempts to have a full-cut splice connection in CFS built-up members for investigating the structural behavior and possible practical application.

Location of the Splice Connection for Built-Up Column Assembly

The splice connections in the built-up column assemblies are to be used for the overlength CFS structural members, which are prone to fail due to global instability. Therefore, the location of the splice connection along the length of the member may significantly influence the structural behavior and failure mode. Furthermore, the primary purpose of this splice connection in a CFS built-up column-to-column is to maintain the column's center of gravity (keeping the section's center of gravity and loading axis closer or make it coincide) and ensure that the column member achieves its design load of the actual column (without a splice connection). With that objective, it is necessary to find an appropriate location (middle of the column or between the middle and end of the column) for the connection between the two individual limbs in the built-up cross-sections. The columns will have higher deflection (flexural or torsional buckling, bend or twist) and moment at the midlength caused by load, an additional effect due to the initial imperfection and inherent eccentricity. Thus, it is not possible to have a splice connection at the high moment region irrespective of the boundary conditions. The appropriate location for splice connection would be the place where the influence of the moment is insignificant; hence, the designer must locate the splice connection prior to the fabrication of the long CFS wall frame.

In the case of a fixed end column, there is an end moment at the supports, a maximum moment at the midlength, and the total unbraced length (distance between zero moment points) is half the

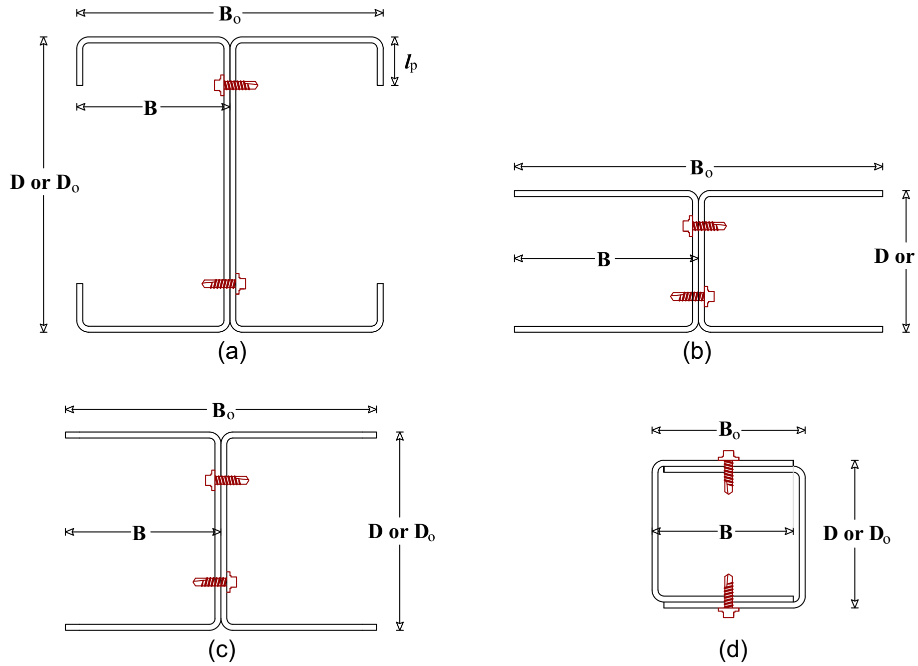

Fig. 3. CFS built-up cross-sections: (a) back-to-back connected lipped channels; (b and c) back-to-back connected unlipped channels; and (d) face-to-face connected unlipped channels.

length ($L/2$ = middle half length of the column); therefore, it will be appropriate to locate the splice connection at the $L/4$ distance from both supports, as shown in Figs. 2(c and d). If a splice connection is provided at an $L/4$ distance from the ends, the maximum length of the single limb in the built-up cross-section will be three-quarters of the overall length of the member, as shown in Fig. 2(d). In the case of the both ends pinned column, the maximum moment is at the middle of the column and zero moments at the supports. However, practically, zero moment at the ends of the CFS wall panel frame is not possible due to the anchoring effect by hold-down connections (with the concrete or steel member) at the supports. Studies by Vieira (2011), Vieira and Schafer (2013), Ye et al. (2016), Serrette and Ogunfunmi (1996), and Serrette et al. (1997) on CFS wall panels have endorsed the same. Therefore, the provision of the splice connection for a built-up member may be placed at an $L/4$ distance from the supports for fixed and pin-end condition columns. One additional advantage in this built-up column assemblies for a splice connection is that there is no need to have a full cut in both the CFS limbs at one location [as shown in Fig. 4(s)]; rather, one limb can be cut at an $L/4$ distance from the bottom support end, while the other can be cut at $L/4$ distance from the top support end, as shown in Fig. 2(d).

Present Investigation

The objective of this present investigation is to experimentally understand the structural behavior of the splice connections in various CFS built-up column assemblies. The adequacy of the splice connections was checked by comparing the strength (both ultimate and design strength) and stiffness (initial slope in load-versus-displacement plot) of the splice connected column and actual column (column without any splice connection). The length of the column tested is limited to the height of the compression testing machine (1,800 mm) used. It is anticipated that the findings of this study will apply to the higher length of the column, as the axial compression strength of the longer column is less than that of the shorter column. Thus, if the proposed splice connection is capable of transferring the compression force in the 1,800 mm length column, then it will also be able to transfer the load in a long column with lesser compressive force.

Twenty-eight built-up columns were tested in this investigation, including four different built-up cross-sections in which the design parameters of the splice connections are varied. In each of the four different cross-sections, an actual column without any splice connection was tested first to understand the overall structural behavior (ultimate strength, initial stiffness, and failure mode). The parameters investigated are mainly the length of the splice (90, 100, 150, 200, and 300 mm), the number of fastener rows (single row and double row), the thickness of the splice (1.5, 2.0, and 2.5 mm), and location of the splice. Although it was decided not to have the splice connection at the midlength of the column, two columns were tested with midsplice connection with two different lengths of the splice for comparison.

The four different built-up cross-sections investigated in this study are shown in Fig. 3 and Table 1 with dimensions. Of the four different cross-sections, three of them are back-to-back connected built-up cross-sections (BBCL-100-50-1.5, BBCU-50-65-1.5, and BBCU-70-50-1.5), and one is of face-to-face connected built-up cross-section (FFCU-50-50-1.5). All the built-up columns tested in this study are 1,800 mm long and with an intermediate fastener spacing of 180 mm ($L/10$). The ratio for the $(a/r_i)/(KL/r)_o$ for all the specimens was less than 0.5 (0.21 to 0.28, as shown in Table 1) according to Section II.2 of AISI 2020. The built-up columns were tested with a fixed-fixed end condition.

Nomenclature for the Experimental Investigation

First, the CFS built-up cross-sections were named based on the geometry (specimen ID in Table 2); for example, the back-to-back connected lipped channel cross-section geometry was named BBCL followed by its full built-up cross-section dimensions

J. Struct. Eng., 2023, 149(3): 04022250

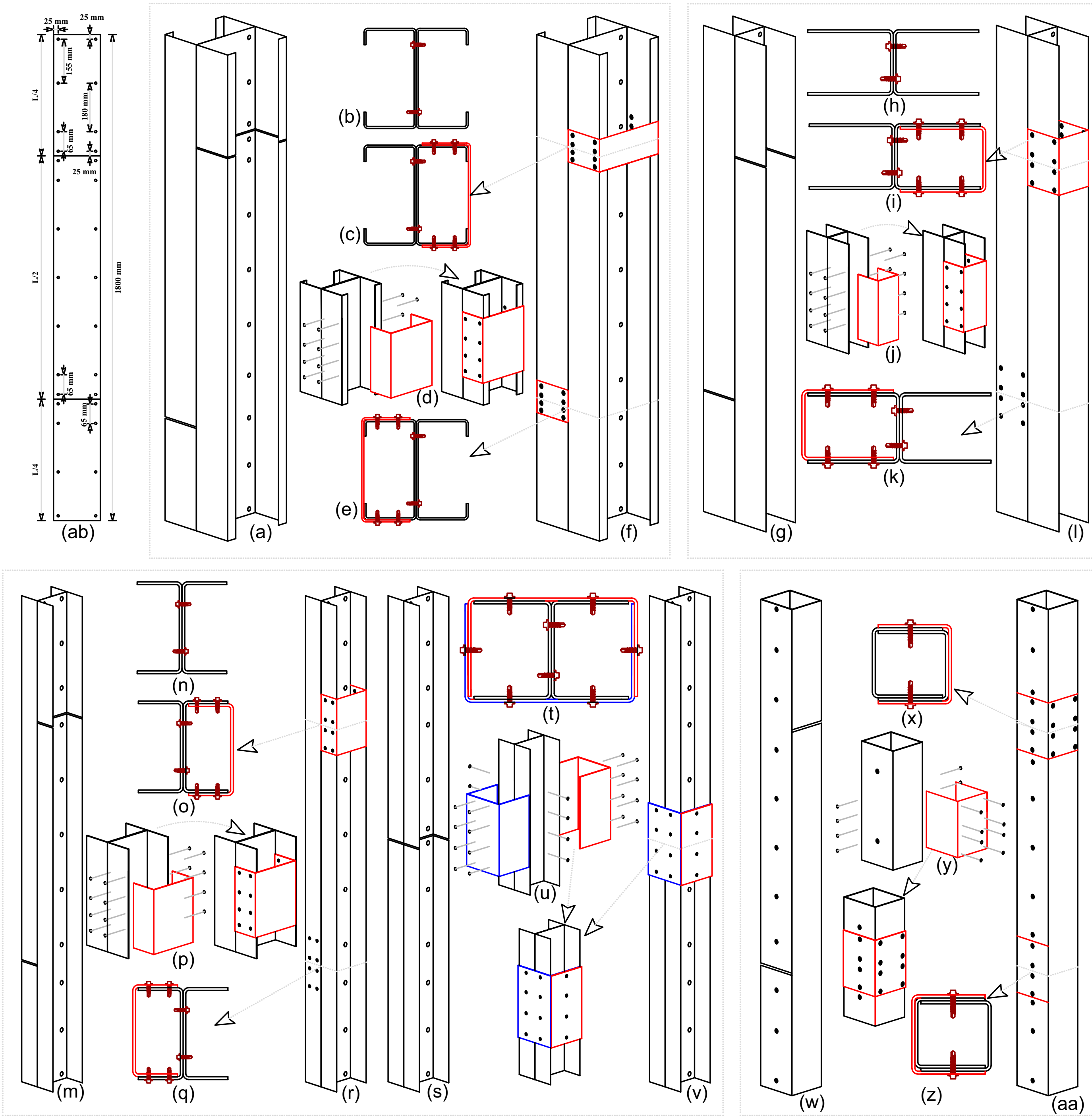

Fig. 4. Splice connection configuration, arrangement, and installation methods for cold-formed steel construction: (a–f) over-size splice for the back-to-back connected lipped channel built-up column assembly; (g–l) same size splice for the back-to-back connected unlipped channel built-up column assembly; (m–r) same size splice for the back-to-back connected unlipped channel built-up column assembly; (s–v) over-size splice at the mid-length for the back-to-back connected unlipped channel built-up column assembly; (w–aa) over-size splice for the face-to-face connected unlipped channel built-up column assembly; and (ab) Dimensions and spacing configuration in the splice connected built-up column.

(i.e., depth, breadth, thickness); similarly, the face-to-face connected unlipped channel cross-section was named as FFCU. The identity "L" and "U" in the column cross-section type indicates the use of lipped and unlipped channels, respectively. The splice connection columns (Splice ID in Table 2) were named based on the length, thickness, and number of fastener rows; for example, the Splice ID "SL-90-1.5-SR" indicates that the length of the splice is 90 mm, thickness is 1.5 mm, and has a single-fastener row. The detailed dimensions of the built-up cross-sections and splice dimensions are summarized in Tables 1 and 2 with corresponding figures.

Built-Up Column Fabrication

The CFS channels for the built-up CFS columns were fabricated from steel sheets by the press brake process. The CFS sheets were

Table 1. Dimensions and slenderness of the CFS built-up column assembly sections

Column type	Figure	Specimen ID	Cross-section dimensions of the individual C channel (mm): Flange (B)	Web (D)	Thickness (t)	Lip (l_p)	Cross section dimensions of the built-up column channel (mm): B-flange (B_o)	B-web (D_o)	Fastener spacing (a): L/a	Actual (mm)	Built-up column length (L) (mm)	$(a/r_i)/(KL/r)_o$
Back-to-back connected lipped channels	Fig. 3(a)	BBCL-100-50-1.5	50	100	1.5	15	100	100	10	180	1,800	0.27
Back-to-back connected unlipped channels	Fig. 3(b)	BBCU-50-65-1.5	65	50	1.5	—	130	50	10	180	1,800	0.21
	Fig. 3(c)	BBCU-70-50-1.5	50	70	1.5	—	100	70	10	180	1,800	0.28
Face-to-face connected unlipped channels	Fig. 3(d)	FFCU-50-50-1.5	50	50	1.5	—	50	50	10	180	1,800	0.23

Note: B = width of the flange of the individual channel cross-section; D = depth of the web of the individual channel cross-section; t = thickness of the CFS channel and built-up cross-section assembly; l_p = lip of the C channel; B_o = width of the flange of the built-up cross-section; D_o = depth of the web of the built-up cross-section; L = length of the built-up member; a = intermediate fastener spacing; r_i = radius of gyration of the individual cross-section; K = effective length factor; and r = radius of gyration of the built-up cross-section.

Table 2. Built-up column assembly sections and corresponding splice connection dimensions

Column cross-section type	Specimen ID	Cross-section dimensions of the built-up column assembly (mm): B-flange (B_o)	B-web (D_o)	Thickness (t)	Splice arrangements: Splice ID	Location[a]	Length (L_s) (mm)	Thickness (mm)	Fastener arrangement (n_f)	Splice figure
Back-to-back connected lipped channels	BBCL-100-50-1.5	100	100	1.5	Control-1	No splice	No splice (disconnected column)			
					Control-2	No splice	No splice (disconnected column)			
					SL-90-1.5-SR	¼ L and ¾ L	90	1.5	Single row	Figs. 4(a–f)
					SL-90-1.5-DR	¼ L and ¾ L	90	1.5	Double row	Figs. 4(a–f)
					SL-150-1.5-DR	¼ L and ¾ L	150	1.5	Double row	Figs. 4(a–f)
					SL-300-1.5-SR	¼ L and ¾ L	300	1.5	Single row	Figs. 4(a–f)
					SL-300-1.5-DR	¼ L and ¾ L	300	1.5	Double row	Figs. 4(a–f)
Back-to-back connected unlipped channels	BBCU-50-65-1.5	130	50	1.5	SL-100-1.5-DR	¼ L and ¾ L	100	1.5	Double row	Figs. 4(g–l)
					SL-150-1.5-DR	¼ L and ¾ L	150	1.5	Double row	Figs. 4(g–l)
					SL-200-1.5-DR	¼ L and ¾ L	200	1.5	Double row	Figs. 4(g–l)
					SL-300-1.5-DR	¼ L and ¾ L	300	1.5	Double row	Figs. 4(g–l)
Back-to-back connected unlipped channels	BBCU-70-50-1.5	100	70	1.5	SL-90-1.5-DR	¼ L and ¾ L	90	1.5	Double row	Figs. 4(m–v)
					SL-90-2.5-DR	¼ L and ¾ L	90	2.5	Double row	Figs. 4(m–v)
					SL-150-1.5-DR	¼ L and ¾ L	150	1.5	Double row	Figs. 4(m–v)
					SL-150-2.5-DR	¼ L and ¾ L	150	2.5	Double row	Figs. 4(m–v)
					SL-300-1.5-DR	¼ L and ¾ L	300	1.5	Double row	Figs. 4(m–v)
					SL-150-2.0-DR	Middle	150	2.0	Double row	Figs. 4(m–v)
					SL-300-2.0-DR	Middle	300	2.0	Double row	Figs. 4(m–v)
Face-to-face connected unlipped channels	FFCU-50-50-1.5	50	50	1.5	SL-90-1.5-DR	¼ L and ¾ L	90	1.5	Double row	Figs. 4(m–v)
					SL-90-2.5-DR	¼ L and ¾ L	90	2.5	Double row	Figs. 4(w–aa)
					SL-150-1.5-DR	¼ L and ¾ L	150	1.5	Double row	Figs. 4(w–aa)
					SL-150-2.5-DR	¼ L and ¾ L	150	2.5	Double row	Figs. 4(w–aa)
					SL-300-1.5-DR	¼ L and ¾ L	300	1.5	Double row	Figs. 4(w–aa)
					SL-300-2.5-DR	¼ L and ¾ L	300	2.5	Double row	Figs. 4(w–aa)

[a]Please see Fig. 2(d) for location details of the splices.

cut to the desired specimen length for press braking. The CFS sheets are of different yield strengths, as summarized in Table 3, with zinc-coating. After the press braking process, two identical CFS channels were connected by two parallel rows of fasteners, as shown in Fig. 3. The fasteners are drilled at a 25 mm distance from the ends of the column followed by a constant intermediate connection spacing (a). To prevent the unthreading of fasteners during buckling, the fasteners are aligned in opposite directions in the same row (alternative), as per Indian industrial practice (as shown in Fig. 3). To further ensure the rigidity of fastener connections, the self-drilling fasteners are drilled such that a minimum of three threads are penetrated through the last steel sheet (NAHB 1997). After forming built-up cross-sections, the ends of the columns were milled (grinding) for the proper welding of column end plates. The dimensions of the end plates were larger by a minimum of 100 mm than the overall column cross-section, and the thickness

J. Struct. Eng., 2023, 149(3): 04022250

Table 3. Material properties of the CFS column and splices

Cold-formed steel component	Thickness	E (GPa)	f_y (MPa)	f_u (MPa)	ε_f
Built-up column assemblies	1.5	202.7	378.3	442.8	18.2
Splices	1.5	202.7	378.3	442.8	18.2
	2.0	211.5	330	425	18
	2.5	214.8	329.6	417.3	18

Note: E = Young's modulus of steel; f_y = yield strength of steel; f_u = ultimate tensile strength; and ε_f = strain at fracture.

was 12 mm. The minimum loading eccentricity (L/1,000) was included in the built-up column specimen by aligning with the end plates before welding. The flatness of the end base plate was ensured by the grit blasting and manual grinding process for full contact with the loading platen.

Material Properties of the CFS Steel Sheets

The material properties of the CFS steel sheets used for the built-up columns were obtained from tensile coupon tests. The tensile coupons were extracted from the steel channels (after the press brake process). The coupon samples were taken from both webs and flanges of the CFS channels using the wire cut process, as shown in Fig. 5(a). The tensile test coupon dimensions conform to the ASTM E8 Standard (ASTM 2013). The tensile coupon test was carried out using an MTS Universal Testing Machine of 100 kN capacity. A constant displacement rate of 0.5 mm/min was applied for the tensile coupon tests with the help of extensometers [Fig. 5(b)]. A data-acquisition system was used to obtain the test readings (load, displacement, and strain). The static loading was achieved by pausing the applied displacement at 0.2% tensile strain and three more points before reaching the ultimate stress. Pausing the applied load will relax the stress in the tensile test coupons. The material properties obtained from the tensile test are summarized, including Young's modulus of steel (E_s), yield strength of steel (f_y), ultimate tensile strength (f_u), and strain at fracture (ε_f) in Table 3.

Test Setup

The axial loading test setup for the built-up column assembly with a splice connection is shown in Fig. 6. The tests were conducted using the Microtest servo-controlled hydraulic compression testing machine. The bottom end platen of the compression testing machine is equipped with a hydraulic piston (move up and down) for displacement control and application. A rigid connection was provided at both ends of the column to ensure fixity by restraining the translation, warping, and rotation. The shim plates (thickness 0.5 mm) were used for ensuring proper seating of columns on the machine's platen. The center of gravity of both the top and bottom end plates is positioned with the center of gravity of the machine's platens. The compression load was applied in displacement control mode at a constant rate of 0.2 mm/min. The axial displacement (shortening) of the column was obtained from the noncontact linear variable displacement transducer (NCDT), which was fitted additionally on top of the machine's bottom platen and the linear variable displacement transducer (LVDT), which is inbuilt with the machine's bottom piston. The loading and corresponding displacement data were acquired by the data-acquisition system at regular intervals. It was observed that the axial shortening measurements using NVDT and inbuilt LVDT are almost the same for all the specimens; only for a few specimens, however, these measurements were varying in the post-peak zone due to sudden instability failure. Therefore, the inbuilt LVDT displacement readings were used for plotting the axial load (kN) versus axial displacement curves for consistency.

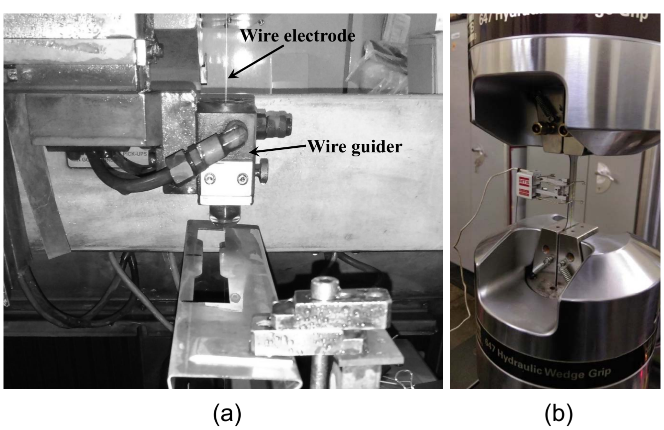

Fig. 5. (a) Wire-cutting process for coupon testing; and (b) testing of CFS coupons in universal testing machine.

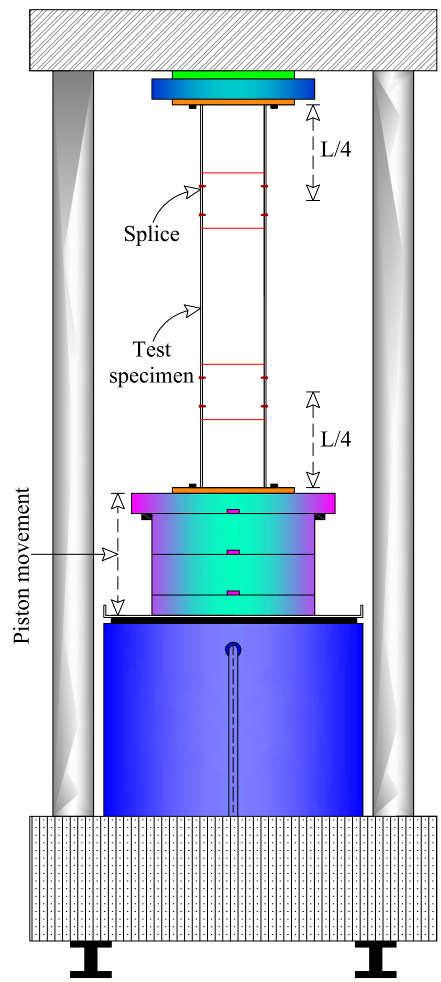

Fig. 6. Test arrangements for compression testing of CFS columns with splice connections.

Results and Discussion

The experimental results, including structural behavior of actual columns, splice connected columns, and splice components, are summarized in Table 4, with corresponding axial load and failure modes. It was observed that the length of the splice (L_s) and the number of fastener rows (n_f) played an influential role in the transfer of force between two disconnected built-up column members. Further, it was observed that the web portion of the splice restrains the flanges of the column from displacement (buckling) and lets the flanges of the splice transfer force between the column flanges. This shows that the individual unstiffened plate type splice connections used in the hot-rolled steel column shown in Fig. 1(a) do not suit the CFS column-to-column connections as the flange and web of the splice need to act together as a stiffening element to each other to control the complex buckling modes of CFS channels. The load-displacement curves, their corresponding failure modes, and the effect of splice connections are shown in Figs. 7–13. The load-displacement curves and failure modes of actual columns, disconnected columns, and columns with splice connections are shown in the same figures for easy comparison.

Actual Column (without Splice) Behavior and Design Strength

Prior to the testing of the built-up column with splice connections, an actual column with no splice connection was tested for all four different built-up cross-sections. The stiffness of the actual columns is shown in Figs. 7(a), 8(a), 9(a), 10(a), and 11(a) (curves with legend "Actual") are stiff until reaching 95% of the ultimate load and the failure modes are global buckling (BBCL-100-50-1.5) and interaction between local and global buckling (BBCU-50-65-1.5, BBCU-70-50-1.5, and FFCU-50-50-1.5).

The failure mode photos of the actual columns, as shown in Figs. 9(b), 10(b), and 11(b), indicate that the load is spread uniformly to the cross-section and the load is transferred fully from both the ends to the middle portion of the column as the local buckling with global interaction occurred near the column's midlength. The design strength (P_{DSM}) of the actual column is calculated using the direct strength method (DSM) (AISI 2020) with a modified global slenderness approach (Section II.2 of AISI 2020) and a modified local slenderness approach (Selvaraj and Madhavan 2022). The modified global slenderness approach applies to back-to-back connected and face-to-face connected built-up cross-section columns, while the face-to-face connected columns require the addition of a modified local slenderness approach for incorporating the effect of intermediate connection spacing to the local-global interactive buckling strength (Selvaraj and Madhavan 2022). The calculated design strengths (P_{DSM}) of the actual columns are shown with the corresponding experimental strength of the column in Table 4. It shows that the AISI's DSM method with modified global and local slenderness approaches are accurately predicting the design strength of the columns. If the splice connected column's

Table 4. Strength comparison of built-up column assembly sections with splice connection arrangements

Column type	Built-up column assembly experimental results: Specimen ID	Built-up column assembly experimental results: Axial load (P_T) (kN)	Design capacity as per AISI S100 (AISI 2020) (P_{DSM}) (kN)	Experimental results of built-up column with splice arrangements: Splice ID	Location[a]	Length (L_s) (mm)	Thickness (mm)	Fastener arrangement (n_f)	Failure modes figures	Axial load ($P_{T\text{-}C}$) (kN)
Back-to-back connected lipped channels	BBCL-100-50-1.5	172.05	167.11	Control-1	No splices	No splices			Fig. 7(b)	54.87
				Control-2	No splices	No splices			Fig. 7(c)	61.16
				SL-90-1.5-SR	¼ L and ¾ L	90	1.5	Single row	Fig. 8(b)	62.40
				SL-90-1.5-DR	¼ L and ¾ L	90	1.5	Double row	Fig. 8(c)	108.39
				SL-150-1.5-DR	¼ L and ¾ L	150	1.5	Double row	Fig. 8(d)	119.74
				SL-300-1.5-SR	¼ L and ¾ L	300	1.5	Single row	Fig. 8(e)	152.25
				SL-300-1.5-DR	¼ L and ¾ L	300	1.5	Double row	Fig. 8(f)	170.18
Back-to-back connected unlipped channels	BBCU-50-65-1.5	95.82	94.93	SL-100-1.5-DR	¼ L and ¾ L	100	1.5	Double row	Fig. 9(c)	39.29
				SL-150-1.5-DR	¼ L and ¾ L	150	1.5	Double row	Fig. 9(d)	51.91
				SL-200-1.5-DR	¼ L and ¾ L	200	1.5	Double row	Fig. 9(e)	85.31
				SL-300-1.5-DR	¼ L and ¾ L	300	1.5	Double row	Fig. 9(f)	97.98
Back-to-back connected unlipped channels	BBCU-70-50-1.5	106	106.22	SL-90-1.5-DR	¼ L and ¾ L	90	1.5	Double row	Fig. 10(c)	37.64
				SL-90-2.5-DR	¼ L and ¾ L	90	2.5	Double row	Fig. 10(d)	51.02
				SL-150-1.5-DR	¼ L and ¾ L	150	1.5	Double row	Fig. 10(e)	54.51
				SL-150-2.5-DR	¼ L and ¾ L	150	2.5	Double row	Fig. 10(f)	63.19
				SL-300-1.5-DR	¼ L and ¾ L	300	1.5	Double row	Fig. 10(g)	107.54
				SL-150-2.0-DR	Middle	150	2.0	Double row	Fig. 10(h)	48.63
				SL-300-2.0-DR	Middle	300	2.0	Double row	Fig. 10(i)	79.22
Face-to-face connected unlipped channels	FFCU-50-50-1.5	96.91	92.23	SL-90-1.5-DR	¼ L and ¾ L	90	1.5	Double row	Fig. 11(c)	41.84
				SL-90-2.5-DR	¼ L and ¾ L	90	2.5	Double row	Fig. 11(d)	43.40
				SL-150-1.5-DR	¼ L and ¾ L	150	1.5	Double row	Fig. 11(e)	42.06
				SL-150-2.5-DR	¼ L and ¾ L	150	2.5	Double row	Fig. 11(f)	65.41
				SL-300-1.5-DR	¼ L and ¾ L	300	1.5	Double row	Fig. 11(g)	93.60
				SL-300-2.5-DR	¼ L and ¾ L	300	2.5	Double row	Fig. 11(h)	98.07

Note: P_T = experimental capacity of the actual built-up columns; P_{DSM} = design capacity of the actual built-up columns as per direct strength method of AISI S100 (AISI 2020); and $P_{T\text{-}C}$ = experimental capacity of the disconnected and splice connected built-up columns.
[a]Please see Fig. 2(d) for location details of the splices.

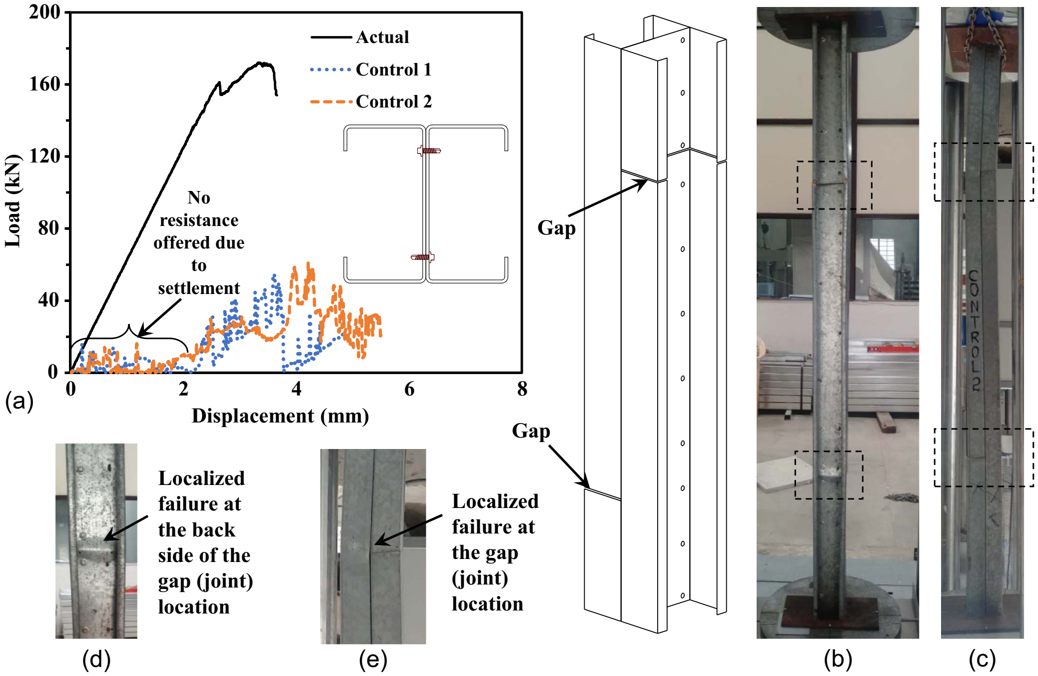

Fig. 7. Structural response and failure modes of CFS back-to-back connected lipped channel built-up column assembly (BBCL-100-50-1.5): (a) load-displacement plot, comparison between actual column (without any cut or connections) and disconnected column; and (b–e) failure modes of disconnected column.

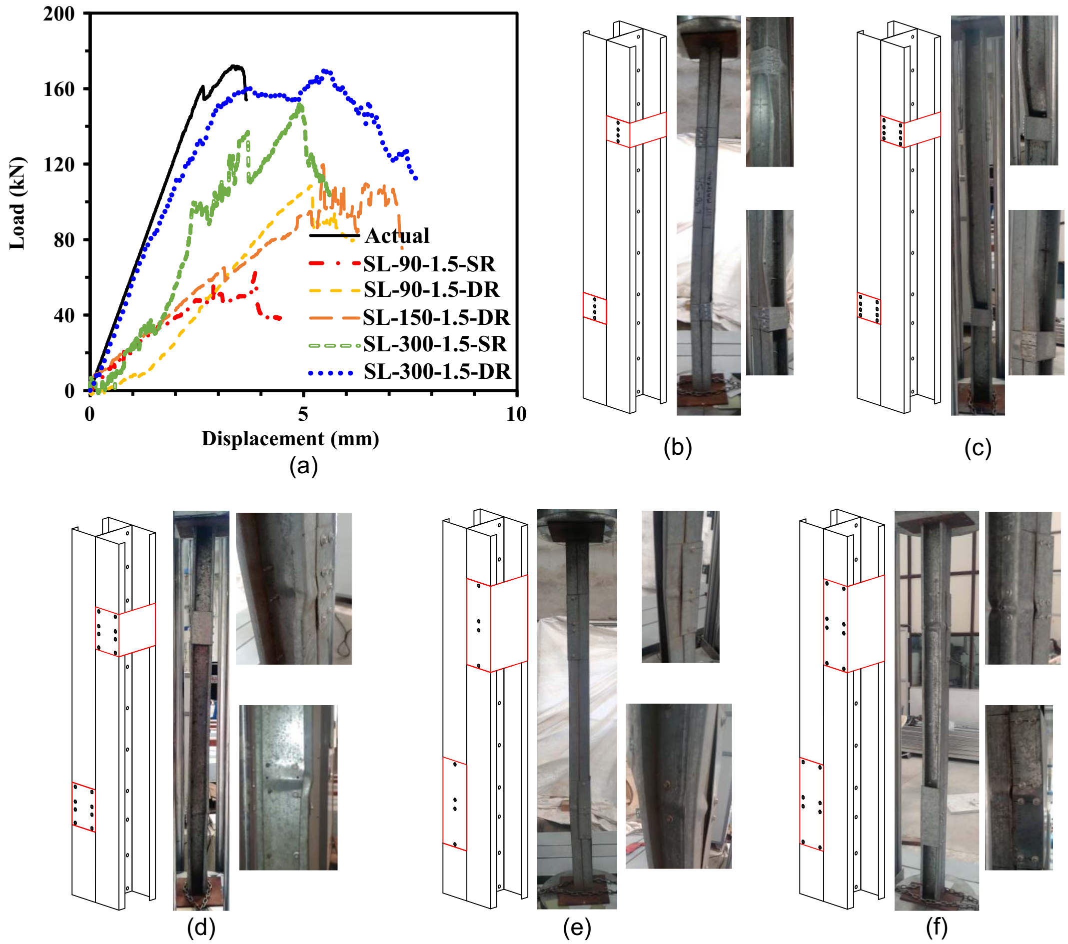

Fig. 8. Structural response and failure modes of CFS back-to-back connected lipped channel built-up column assembly (BBCL-100-50-1.5): (a) load-displacement plot, comparison between actual column (without any cut or connections) and splice connected columns; (b) SL-90-1.5-SR; (c) SL-90-1.5-DR; (d) SL-150-1.5-DR; (e) SL-300-1.5-SR; and (f) SL-300-1.5-DR failure modes of splice connected CFS columns.

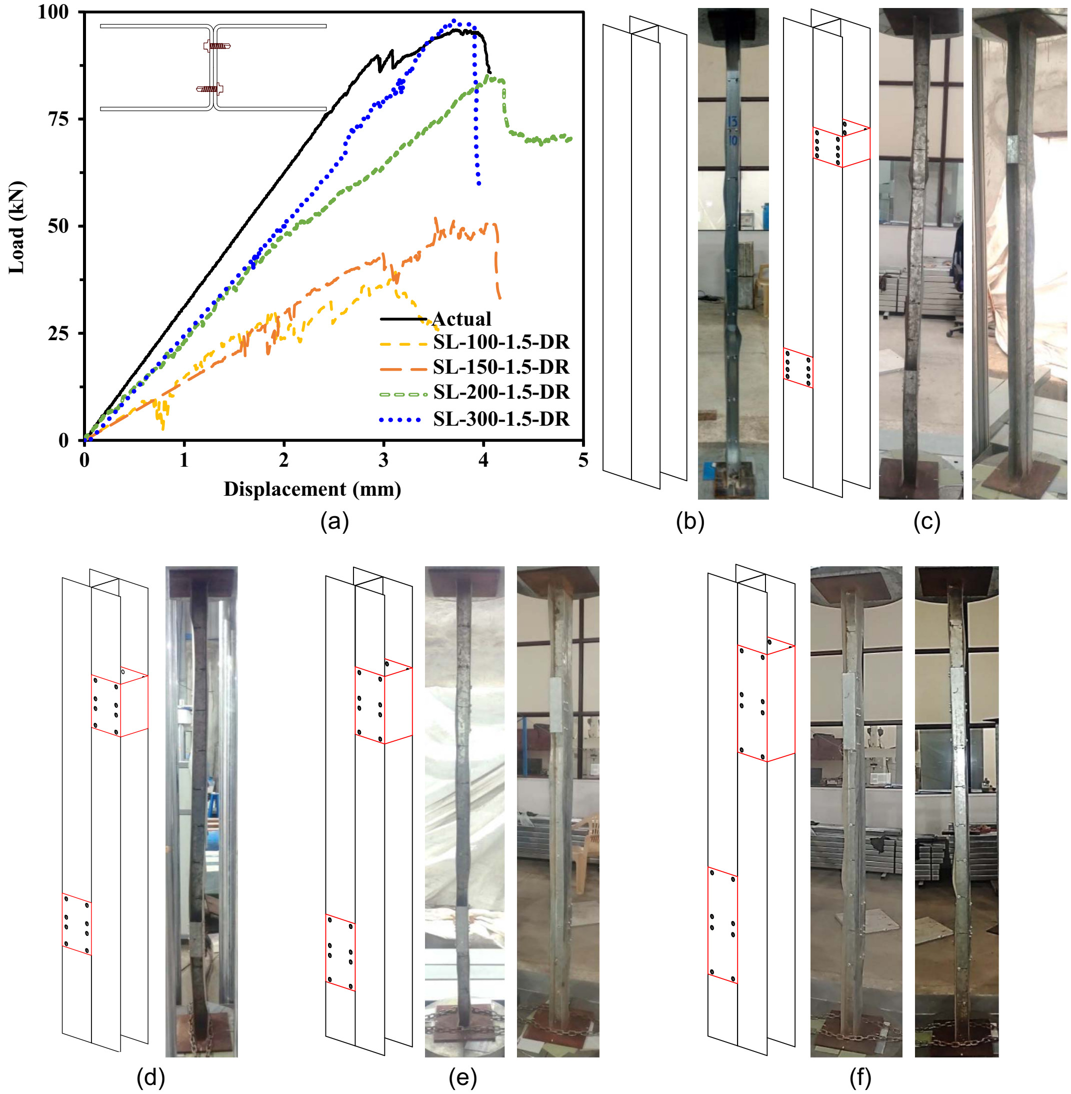

Fig. 9. Structural response and failure modes of CFS back-to-back connected unlipped channel built-up column assembly (BBCU-50-65-1.5): (a) load-displacement plot, comparison between actual column (without any cut or connections) and splice connected columns; (b) failure mode of actual column; (c) SL-100-1.5-DR; (d) SL-150-1.5-DR; (e) SL-200-1.5-DR; and (f) SL-300-1.5-DR failure modes of splice connected CFS columns.

ultimate experimental strength ($P_{T\text{-}C}$) is higher than the corresponding actual column design strength (P_{DSM}), then it can be assumed that the provided splice connection configuration is sufficient for load transfer.

Disconnected Column (without Connection)

The column with disconnection at one-fourth L distance from both ends was tested (two samples, Splice ID, "Control 1" and "Control 2") for checking the structural behavior, as shown in Fig. 7. The specimens did not resist the load at the initial stage [marked in Fig. 7(a)]; after the application of 2 mm axial displacement (settlement), however, they started resisting the load; moreover, the local failure occurred at the cut locations, as shown in Figs. 7(b–e). Though there is a cut between the two individual limbs, the specimens were resisting up to 54.87 kN ($P_{T\text{-}C}/P_{DSM} = 0.33$) and 61.17 kN ($P_{T\text{-}C}/P_{DSM} = 0.37$), respectively. This late resistance offered by the disconnected columns may be attributed to the fact that the web portion of the individual limbs is already well connected with each other with two rows of fasteners, which can distribute the force between the members to some extent. However, the failure occurred due to the buckling of the flange in the continuous limb [Fig. 7(d)], resulting in a bent toward the discontinuity side, as shown in Fig. 7(e).

Influence of Various Design Parameters of Splice Connections

Having understood the structural behavior of the actual column, i.e., its design strength, disconnected column, and its structural behavior, the four different built-up column cross-section assemblies with the splice connections were investigated with various design parameters (length of the splice, splice location, plate thickness, and fastener arrangement).

Back-to-back connected lipped channels built-up cross-section assembly: First, BBCL-100-50-1.5 specimens with splice connections were tested. The specimen with a 90 mm splice connection and a single row of fasteners (SL-90-1.5-SR) attained 62.4 kN,

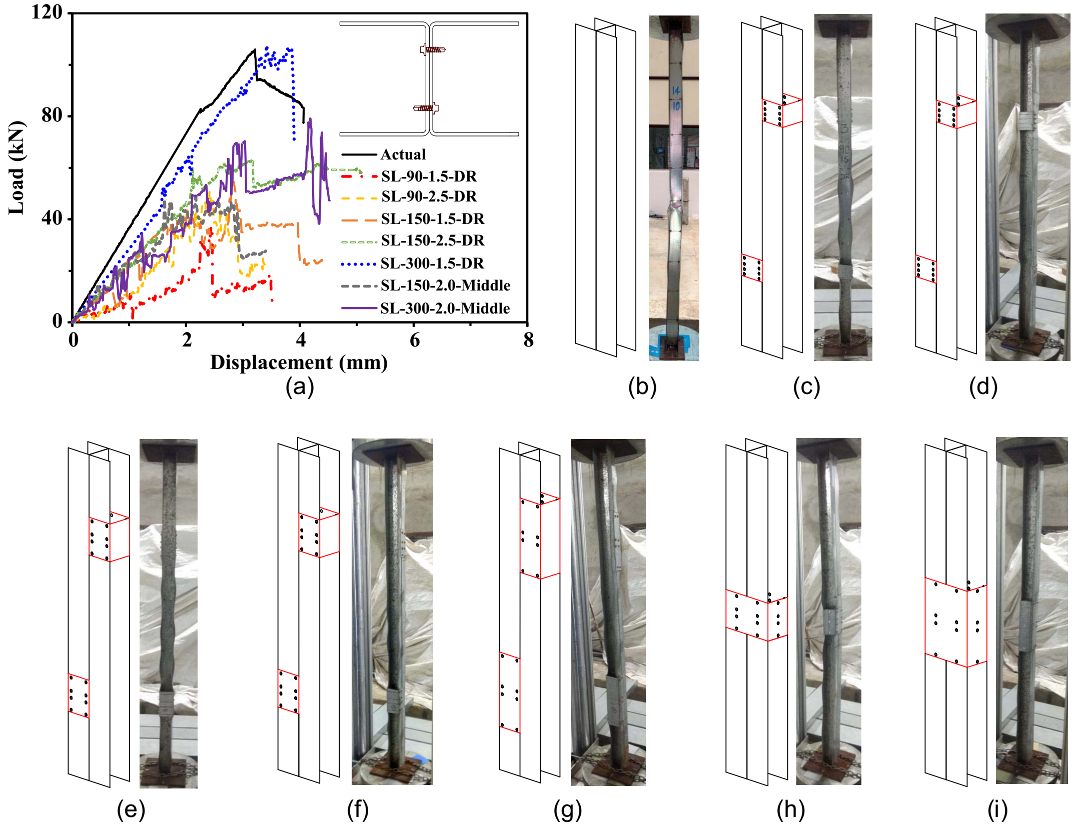

Fig. 10. Structural response and failure modes of CFS back-to-back connected unlipped channel built-up column assembly (BBCU-70-50-1.5): (a) load-displacement plot, comparison between actual column (without any cut or connections) and splice connected columns; (b) failure mode of actual column; (c) SL-90-1.5-DR; (d) SL-90-2.5-DR; (e) SL-150-1.5-DR; (f) SL-150-2.5-DR; (g) SL-300-1.5-DR; (h) SL-150-2.0-middle; and (i) SL-300-2.0-middle failure modes of splice connected CFS columns.

which is 37.3% of the design capacity of the built-up cross-section (P_{DSM} of BBCL-100-50-1.5 is 167.11 kN), and the failure mode is outward distortional buckling near the splice connections, as shown in Fig. 8(b). The next specimen SL-90-1.5-DR is with a 90 mm splice length and two rows of fastener connections, which attained (108.39 kN) 64.86% of the P_{DSM} of BBCL-100-50-1.5. Though this strength is higher than that of the single-row fastener splice (SL-90-1.5-SR), there is no improvement in the failure mode in SL-90-1.5-DR (distortional buckling near the splices) compared with the SL-90-1.5-SR, as shown in Figs. 8(b and c). This indicates that, even though the two rows of fasteners improved the strength, the stiffness and failure modes did not improve compared with those of single-row fasteners (compare load versus displacement curve and failure modes of SL-90-1.5-SR and SL-90-1.5-DR in Fig. 8). In the next specimen, the length of the splice was increased to 150 mm with two rows of fasteners (SL-150-1.5-DR). This specimen's ultimate load was 119.74 kN, which is not a significant improvement compared with the 90 mm splice with two rows of fasteners; the failure mode also did not improve, with localized failure at the splice connection location [Fig. 8(d)]. The built-up cross-section column with a splice of 300 mm length and single-row fastener (SL-300-1.5-SR) improved the ultimate strength, but the failure mode is not desirable. The SL-300-1.5-SR specimen failed in localized flexural buckling of the single limb, as shown in Fig. 8(e). This indicated that the splice configuration of 300 mm length and a single row of the fastener are not sufficient for attaining the strength equal to the actual column. In the next specimen, with the same 300 mm length of the splice, the number of fasteners is increased to two rows (SL-300-1.5-DR). After adding an additional row of fasteners in a 300 mm splice, the column strength increased to 170.18 kN ($P_{T\text{-}C}$); there is no nonuniform failure at the splice location, as shown in Fig. 8(f). Both the individual channels in the built-up cross-section of SL-300-1.5-DR are buckled simultaneously with the almost same pattern (outward displacement of the flange and inward movement of the web at the splice location) and with no significant global buckling. This combined effect of longer length splice and two rows of fasteners is necessary for the uniform force transfer between one member to the other. The two rows of fasteners keep the flanges of the splice intact with the column flanges and enable force transfer without distortional buckling [Fig. 8(f)], while the single row of fasteners could not resist the buckling of the element, as shown in Fig. 8(e). This indicates that the 300 mm splice connection with two rows of fasteners is sufficient for force transfer between the two connecting limbs of a built-up member.

The above interpretation pertaining to the structural behavior of the splice connections indicates the following: (1) the fastener connections in the flange portion of the splice transfer the load (Figs. 12 and 13); (2) the web portion of the splice restrains the displacement of the individual channel flanges of the built-up cross-section (Fig. 13); (3) as the length of the splice increases, the constraining length increases (overlapping with the fastener connection); therefore, the adequacy of the splice connection increases; and (4) two rows of fastener connection are necessary to keep the splice element intact with the column flanges (Fig. 13).

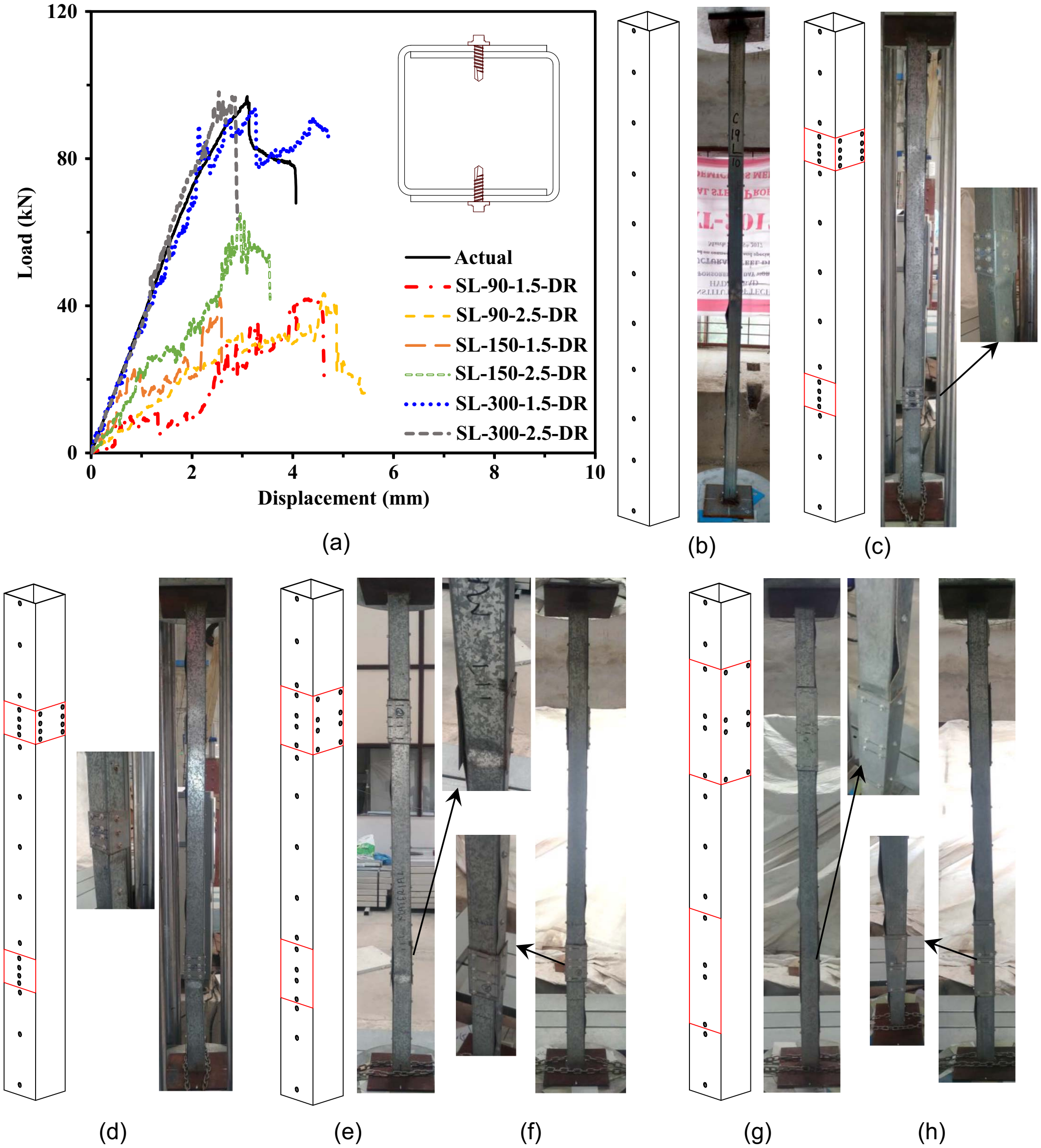

Fig. 11. Structural response and failure modes of CFS face-to-face connected unlipped channel built-up column assembly (FFCU-50-50-1.5): (a) load-displacement plot, comparison between actual column (without any cut or connections) and splice connected columns; (b) failure mode of actual column; (c) SL-90-1.5-DR; (d) SL-90-2.5-DR; (e) SL-150-1.5-DR; (f) SL-150-2.5-DR; (g) SL-300-1.5-DR; and (h) SL-300-2.5-DR failure modes of splice connected CFS columns.

The load transfer effect of the splice connection is depicted in Figs. 12(c and d).

Back-to-back connected unlipped channels built-up cross-section assembly: The next set of specimens are of back-to-back connected unlipped channels (BBCU-50-65-1.5) in which four different splice lengths are tested with two rows of fasteners. The structural behavior and influence of splice (force transfer and constraining effect) are similar to those of the previous set of specimens in BBCL-100-50-1.5. The results of different splice length variations (SL-100-1.5-DR, SL-150-1.5-DR, SL-200-1.5-DR, and SL-300-1.5-DR) in the BBCU-50-65-1.5 specimen set indicate that a minimum of 300 mm length splice with two fastener rows is required for uniform transfer of force in the built-up cross-sections. This can be observed in Fig. 9, where only the SL-300-1.5-DR specimen (97.98 kN) reached the load beyond P_{DSM} (94.93 kN). It should be noted that all the tested splices in a specimen set, i.e., BBCL-100-50-1.5 and BBCU-50-65-1.5, are of 1.5 mm thickness. To further investigate the effect of thickness of splice, the next set of specimens, i.e., BBCU-70-50-1.5, were tested with various thicknesses. The built-up column cross-sections were tested with two thicknesses of splices 1.5 and 2.5 mm, but the difference between 1.5 and 2.5 mm thick splices of 90 and 150 mm is not significant (compare SL-90-1.5-DR versus SL-90-2.5-DR and SL-150-1.5-DR versus SL-150-2.5-DR in Table 4) in terms of failure modes and strength improvements, as shown in Fig. 10. Only the 300 mm length splice with 1.5 mm thickness and two rows of fasteners (SL-300-1.5-DR; $P_{T\text{-}C} = 107.54$ kN) attained the required design load ($P_{DSM} = 106.22$ kN).

Face-to-face connected unlipped channels built-up cross-section assembly: In addition to the difference in the cross-section shape, the main difference between the fabrication of back-to-back and face-to-face connected built-up cross-sections is that, in the former,

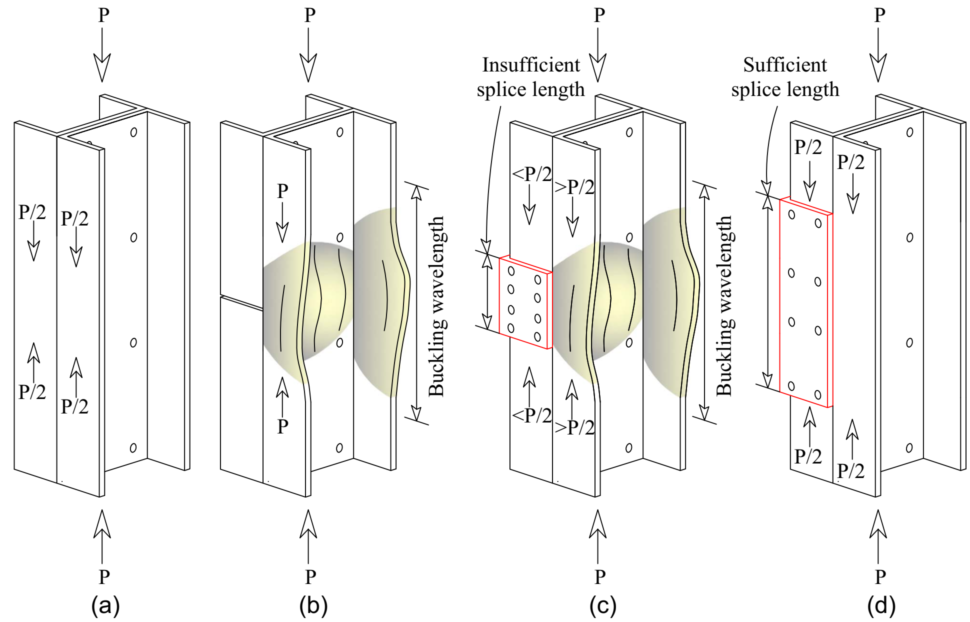

Fig. 12. Influence and effectiveness of the splice connections in the built-up columns: (a) force transfer in the actual column; (b) force transfer in the disconnected column; (c) effect of smaller length splice; and (d) effect of longer length splice.

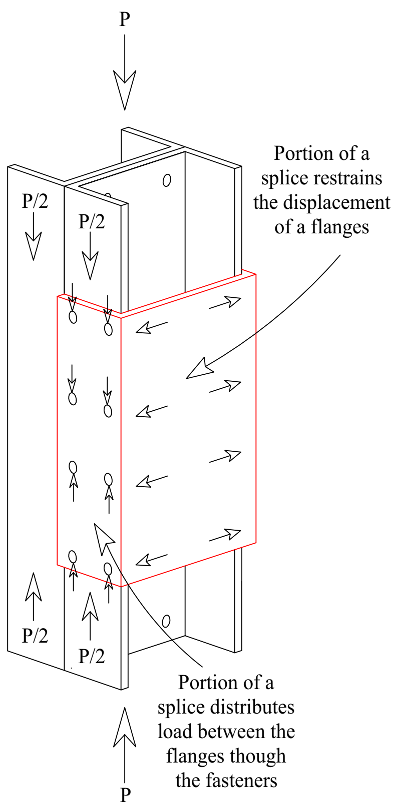

Fig. 13. Force transfer and the constraining effect of the splice in the built-up column-to-column connections.

only the webs are connected by a fastener [Figs. 3(a–c): only one element in each cross-section is connected]; in the latter flanges, both channels are connected [Fig. 3(d): the flanges in individual cross-sections are connected]. Due to the presence of two flange fastener connections in face-to-face connected cross-sections, it is expected that the smaller length of the splice may be enough to increase the stability and force transferring ability of the closed built-up cross-sections. However, this expectation was not true, as only the specimens with 300 mm splice {SL-300-1.5-DR = 93.60 kN and SL-300-2.5-DR = 98.07 kN [Fig. 11(a)]} were able to attain the required design load (P_{DSM} of FFCU-50-50-1.5 = 92.23 kN) (Table 4). It should also be noted that, even the higher thickness splices of 2.5 mm thickness in 90 and 150 mm length could attain only up to 47% and 71% of the design load [Table 4 and Fig. 11(a); compare SL-90-2.5-DR versus SL-150-2.5-DR]. In addition, the difference between the 1.5 and 2.5 mm thickness splices in 300 mm length is less than 5%, indicating that the length of the splice (constraining length) is more effective than the thickness of the splice. The failure modes of FFCU-50-50-1.5 set specimens are shown in Fig. 11.

Splice at the midlength height of the column: Having discussed the efficacy of the length and thickness of the splice, the provision of a splice at the midlength was also investigated. The midlength splice was introduced in the BBCU-70-50-1.5 set specimens. Here, the built-up cross-section was fully cut and joined by the splice, as shown in Figs. 4(s–v). Therefore, to increase the cross-section integrity, the splices were joined perpendicular to the intermediate fastener connections, as shown in Figs. 4(t and u). The midlength connection test results indicate that the constraining effect of 150 mm (SL-150-2.0-DR) and 300 mm (SL-300-2.0-DR) splice with 2 mm thickness is not sufficient for force transfer between the built-up members. This can be observed from load-displacement curves with significant loss and gain in stiffness followed by sudden load drop [Fig. 10(a)] with global failure [Figs. 10(h and i)].

Considerations for Practical Application

The above interpretations pertaining to the structural response and failure modes of the splice connections in CFS built-up columns with various parameters can be summarized as follows for practical implementation:

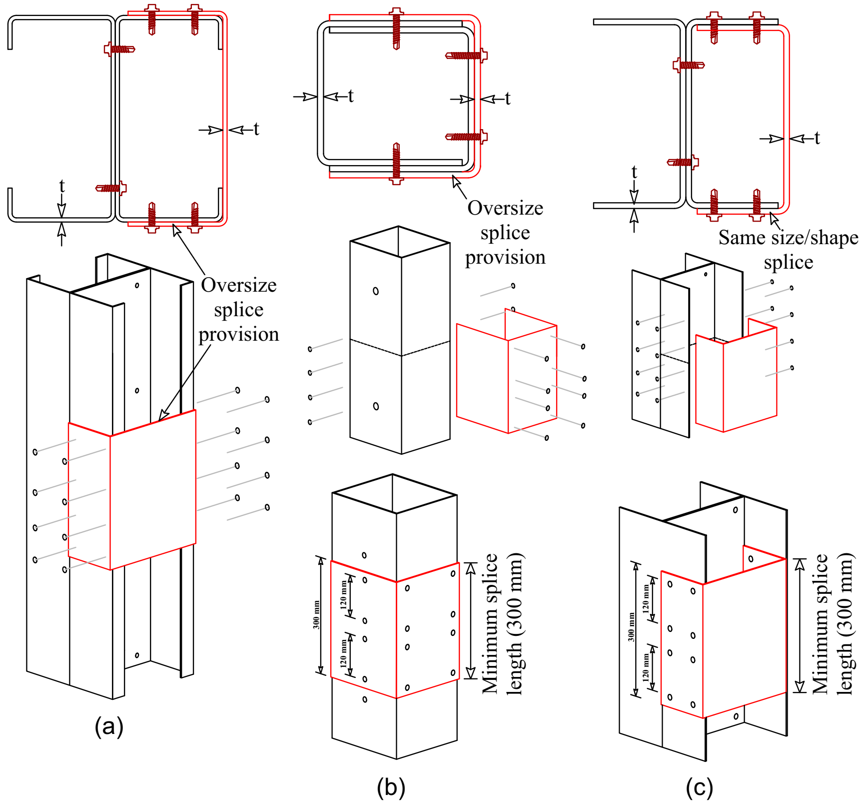

Fig. 14. Recommendations for the splice configuration in column-to-column connections in built up column assembly.

1. The length of the splice connection shall be a minimum of 300 mm for back-to-back and face-to-face connected CFS built-up column cross-sections [Figs. 14(b and c)]. The cross-section dimensions of the splice should be the same as the cross-section dimensions of the built-up column [Fig. 14(c)] or oversized splices [Figs. 14(a and b)] with similar geometry for simple assembly.
2. The location of the joint or splice connection shall not be at the midlength of the column (high moment and large displacement region). However, the column connection should be configured such that one splice is at L/4 distance from one end, and the other splice is provided at L/4 distance from the other end [Figs. 2(d) and 4(a and b)]. This is to ensure that the built-up column is not fully cut or joined at one location.
3. As observed from the 24-splice connected built-up column test results, the thickness of the splice connection does not significantly influence the strength and failure modes of the built-up-column cross-section; nevertheless, it is ascertained that the minimum splice thickness shall be equal to the column cross-section.
4. To have uniform force transfer between the built-up column and constrain the flanges of the built-up cross-sections from buckling, it is suggested to provide two rows of fastener connections.

It should be noted that the aforementioned suggestions are limited to the column cross-sections and length studied in this investigation. The splice configurations used for the shorter column may also apply to longer columns due to lower axial compression strength. However, further investigations are required on various cross-sections with different slenderness ratios to confirm this hypothesis.

Conclusions

An experimental investigation of the structural behavior and strength of built-up columns with splice connections consisting of different cross-sectional dimensions, splice locations, thickness of the splice, and a number of fastener rows are presented in this paper. The new splice connection method for the built-up members in the CFS construction is demonstrated in the form of detailed drawings. The behavior of actual columns and disconnected columns is tested first to compare the behavior and adaptability of the new splice connections. The structural adequacy of the splice connections is verified by comparing the strength of the splice connected columns ($P_{T\text{-}C}$) with the design strength (P_{DSM}) of the corresponding actual columns. The test results indicate that the increase in splice length with two rows of fastener connections increases the adequacy of the force transfer between the two built-up column cross-sections. It was discovered that the increase in thickness of the splice connection is less effective than increasing the splice length. It is profoundly suggested not to use the traditional flat plate splice connections, which are typically used in the hot rolled steel column construction, as the splice connection concept for CFS connection necessitates the integration between web and flange of the splice; the flanges of the splice connections transfer the load through the fastener connections, and the web portion constrains the buckling of the built-up cross-sections. Based on the observed structural behavior and failure modes, a set of recommendations for practical implementation is summarized. The suggested splice connection concept should use the same size and shape of the CFS channel as the built-up column cross-section for ease of connection installation.

Data Availability Statement

All data, models, or code generated or used during the study appear in the published article.

References

AISI (American Iron and Steel Institute). 2020. *North American cold-formed steel specification for the design of cold-formed steel structural members*. AISI-S100-2020. Washington, DC: AISI.

ASTM. 2013. *Standard test methods for tension testing of metallic materials*. E8/E8M-13a. West Conshohocken, PA: ASTM.

Dubina, D., and V. Ungureanu. 2010. "Behaviour of multi-span cold-formed Z-purlins with bolted lapped connections." *Thin-Walled Struct.* 48 (10–11): 866–871. https://doi.org/10.1016/j.tws.2010.04.003.

Ho, H. C., and K. F. Chung. 2006. "Structural behavior of lapped cold-formed steel Z sections with generic bolted configurations." *Thin-Walled Struct.* 44 (4): 466–480. https://doi.org/10.1016/j.tws.2006.03.012.

Liu, J., L. Xu, and S. Fox. 2015. "Lapped cold-formed steel Z-shaped purlin connections with vertical slotted holes." *J. Constr. Steel Res.* 107 (Apr): 150–161. https://doi.org/10.1016/j.jcsr.2015.01.020.

NAHB (National Association of Home Builders). 1997. *Research commentary on the prescriptive method for residential cold-formed steel framing, prepared for the US Department of Housing and Urban Development and American Iron and Steel Institute*. Upper Marlboro, MD: NAHB Research Center, Inc.

NIST (National Institute of Standards and Technology). 2016. *NEHRP seismic design technical brief no. 12—Seismic design of cold-formed steel lateral load-resisting systems—A guide for practicing engineers*. NIST GCR 16-917-38. Gaithersburg, MD: NIST.

Selvaraj, S., and M. Madhavan. 2022. "Design of cold-formed steel built-up closed section columns using direct strength method." *Thin-Walled Struct.* 171 (Feb): 108746. https://doi.org/10.1016/j.tws.2021.108746.

Serrette, R., and K. Ogunfunmi. 1996. "Shear resistance of gypsum-sheathed light-gauge steel stud walls." *J. Struct. Eng.* 122 (4): 383–389. https://doi.org/10.1061/(ASCE)0733-9445(1996)122:4(383).

Serrette, R. L., J. Encalada, M. Juadines, and H. Nguyen. 1997. "Static racking behavior of plywood, OSB, gypsum, and fiber bond walls with metal framing." *J. Struct. Eng.* 123 (8): 1079–1086. https://doi.org/10.1061/(ASCE)0733-9445(1997)123:8(1079).

Vieira, L. C. M., Jr. 2011. "Behavior and design of cold-formed steel stud walls under axial compression." Ph.D. dissertation, Dept. of Civil Engineering, Johns Hopkins Univ.

Vieira, L. C. M., Jr., and B. W. Schafer. 2013. "Behavior and design of sheathed cold-formed steel stud walls under compression." *J. Struct. Eng.* 139 (5): 772–786. https://doi.org/10.1061/(ASCE)ST.1943-541X.0000731.

Ye, J., R. Feng, W. Chen, and W. Liu. 2016. "Behavior of cold-formed steel wall stud with sheathing subjected to compression." *J. Const. Steel Res.* 116 (Jan): 79–91. https://doi.org/10.1016/j.jcsr.2015.08.028.

Zhang, L., and G. Tong. 2008. "Moment resistance and flexural rigidity of lapped connections in multi-span cold-formed Z purlin systems." *Thin-Walled Struct.* 46 (5): 551–560. https://doi.org/10.1016/j.tws.2007.10.010.